Polymer Chain Dynamics and Dynamic Surface Force Apparatuses

Jean-Pierre Montfort

Institut Pluridisciplinaire de Recherche sur l'Environnement et les Matériaux, Université de Pau et des Pays de l'Adour, 2, avenue du Président Angot, 64013 Pau-France

Received December 21, 2007; Revised Manuscript Received March 12, 2008

ABSTRACT: We propose a method for analyzing dynamic experiments done by means of surface force apparatuses on layers of end-grafted or adsorbed layers separated by a compatible polymer melt. We postulate a continuous variation of viscoelastic properties as a function of distance z to the plane. Focusing on small amplitude oscillations, the local behavior is described by a complex shear modulus $G^*(\omega, z)$. In that context, we establish the solution of squeezing flow between plane and sphere. We apply it first to a five-layer configuration made of two layers stuck to the solid surfaces and an intermediate polymer melt separated from the layers by two connecting zones or interfaces. We discuss the results in the framework of tube models, including reptation and tube renewal. We compare them to the situation where the connecting zones are replaced by slipping planes. When the separation between the two surfaces is lower than the thickness of both layers, we solve Navier's equation for describing the compression of the inner part of the layers. The solution is compared to the static force profile obtained from static experiments. The overall complex modulus encompasses the viscoelastic behavior of both inner and outer parts of the gap and the elastic contribution of the inner part made of overlapped and tethered chains. Each part of the expression can be discriminated from the others, allowing experimentalists to play with the structural parameters of both free and tethered chains as well as with grafting density.

1. Introduction

Many experimental and theoretical studies have been conducted on the conformation and dynamics of polymer chains interacting with a surface. The chains are either chemically grafted onto the surface or irreversibly adsorbed, which results in different monomer profiles away from the surface: a steplike profile with a parabolic shape at the free end of the grafted chain in the brush regime,[1] a power-law decaying profile for adsorbed polymers.[2,3] For anchored polymer layers in contact with a compatible polymer melt, the degree of interpenetration between the surface layer and the bulk polymer system is a key parameter. The interaction between end-grafted chains in the brush regime and a polymer melt has been theoretically described.[4,5] Different regimes of brush conformation are predicted as a function of both chain lengths and grafting density. On the other hand, the penetration of free chains inside the brush layer defines a transition zone or interface. The penetration length has been evaluated,[6,7] and even for high grafting densities where the brushes are very stretched, neutron reflectivity experiments show a penetration higher than predicted in the models.[8] Along the same lines, a very recent simulation work[9] has investigated the entanglement density for a polymer brush in contact with a polymeric matrix. It shows an increasing phase separation as the surface coverage increases and at the same time an increase of brush−melt interactions in the crossover region. Models of chain dynamics have been proposed for grafted or adsorbed layers of polymer in presence of good solvent. The solvent swells the chains and is dragged through the network of the anchored chains, creating a viscous dissipation and an elastic strain of the polymer.[10,11] For brush−melt pairs, theoretical[12] and experimental[13] works have been conducted under flow. They study the interfacial friction which plays an important role in adhesion and friction and leads to a slippage at the interface. However, so far no systematic studies have been devoted to the linear viscoelasticity of such complex fluids.

Among the techniques available for investigating the dynamics of confined polymers, new versions of surface force apparatuses have been developed over the last 2 decades. An interesting review by P. F. Luckham and S. Manimaaran[14] describes the improvements brought to the traditional equipment as well as a new concept of machine.[15] Moreover, dynamic nanoindentors can be adapted as nanorheometers. In the same review, the authors report a great number of experiments mainly conducted with adsorbed or grafted polymer layers in presence of solvent. But very few are dealing with polymer layers interacting with free polymer chains and less few present frequencies scan of the viscoelastic properties of such complex systems.[16] Yet, such a mechanical spectrometry is a powerful tool for investigating the details of their dynamics and for discriminating the various components of the relaxation spectrum. The behavior of tethered chains is different from that of free chains and it will be affected by their interconnection degree.

The aim of this paper is to provide the conceptual framework for analyzing experimental data obtained for such complex fluids with dynamic surface force apparatuses. Here we are dealing with heterogeneous polymer systems confined between plane and sphere and submitted to small axial oscillations around a mean separation h_0 between the two surfaces. The measured force reveals the global viscoelastic behavior of the gap close to equilibrium and it is driven by the dynamics of the individual chains. Therefore, the goal is how to deduce the local properties from the global measure of a dynamic force at various surface separations.

We will essentially investigate the situation of symmetric interactions: both surfaces are covered by adsorbed or grafted layers of polymer and separated by a concentrated solution of polymer or a polymer melt. The first section deals with nonoverlapping layers. The distance between the two surfaces is larger than the thickness of the two layers and the behavior of the confined fluid can be either purely viscous or viscoelastic. The second section will be devoted to overlapped layers described as elastic or viscoelastic solids in the central zone of the gap. We will mention in Appendix B how to treat the case of asymmetric surfaces.

2. Nonoverlapping Layers

As sketched in Figure 1, the geometry of surface force machines is a space between plane and sphere with a separation

10.1021/ma7028488 CCC: $40.75
Published on Web 05/17/2008

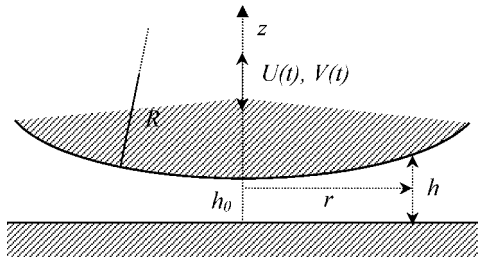

Figure 1. Sketch of the geometry of surface force apparatuses. Derjaguin's approximation ($R \gg h_0$) is fulfilled, and the upper sphere is moved with amplitude $U(t) \ll h_0$.

h_0 much lower than the radius R of the sphere (Derjaguin's approximation). Therefore, the local separation h at distance r from the axis satisfies:

$$h \approx h_0 + r^2/2R$$

An axial motion imposed to the sphere with a velocity $V(t)$—and displacement $U(t)$—induces a normal force $F(R, h_0, V)$ on the plane, via the confined fluid. The plane is supposed fixed and no slippage occurs between the fluid and the non deformable surfaces. As the flow will primarily occur in the radial direction, some approximations can be made on the velocity field inside the fluid: $\partial/\partial z \gg \partial/\partial r$, v_z mainly depends on z, and $v_r \gg v_z$.

2.1. Homogeneous and Newtonian Fluids. This is the basic situation of squeezing flow well described in the literature.[17] The main simplified equations are as follows.

The constitutive equation:

$$\tau_{rz} = \eta \frac{\partial v_r}{\partial z} \tag{1}$$

The motion equation:

$$\frac{dP}{dr} = \frac{\partial \tau_{rz}}{\partial z} = \eta \frac{\partial^2 v_r}{\partial z^2} \tag{2}$$

The continuity equation:

$$\frac{1}{r}\frac{\partial}{\partial r}(r v_r) + \frac{\partial v_z}{\partial z} = 0 \tag{3}$$

They lead to the following lubrication force (calculations in Appendix A.I):

$$F(R, h_0, V) = \frac{6\pi R^2 \eta V}{h_0} \tag{4}$$

The sign of the force is defined with respect to the orientation of the z-axis and not as an interaction force, i.e., with a positive sign when the force is repulsive and conversely.

A modification of the above force coming from possible slippage between the fluid and the surfaces has been described by Vinogradova.[18] An extrapolation length b is defined as the distance to the surface where v_r is zero. At low velocity, that parameter b is constant and the expression of the hydrodynamic force is modified in this way:

$$F(R, h_0, b, V) = \frac{2\pi R^2 \eta V}{b}\left[1 - \left(1 + \frac{h_0}{6b}\right)\ln\left(1 + \frac{6b}{h_0}\right)\right] \tag{5}$$

2.2. Homogeneous and Viscoelastic Fluids. It as been shown[19] that eq 4 can be extended to simple viscoelastic liquids for which the constitutive equation obeys:

$$\eta \frac{\partial v_r}{\partial z} = \tau_{rz} + \frac{\eta}{G}\dot{\tau}_{rz} \tag{6}$$

with G being the shear modulus.

For oscillatory experiments, we use complex notations: $a^*(t) = a^* \exp(i\omega t)$. Therefore, eq 6 can be written as:

$$\tau_{rz} = \eta^* \frac{\partial v_r^*}{\partial z} \tag{7}$$

with the complex viscosity:

$$\eta^* = \frac{\eta}{1 + i\omega\frac{\eta}{G}} \tag{8}$$

The ratio $\eta/G = \eta J$ is a characteristic or relaxation time λ of the fluid.

Taking the remaining relations between complex viscosity, modulus, and compliance

$$G^*(\omega) = i\omega\eta^*(\omega) = 1/J^*(\omega) \tag{9}$$

the above results (section 2.1) can be extended to complex quantities and lead to

$$F^*(R, h_0, \omega) = \frac{6\pi R^2 \eta^*(\omega, h_0) V^*}{h_0} = \frac{6\pi R^2 U^*}{h_0} G^*(\omega, h_0) \tag{10}$$

The measured force is directed connected to the global viscoelastic behavior of the gap via the complex shear modulus. However, so far, the details of the fluid dynamics have been ignored.

2.3. Heterogeneous Fluid. As the confined fluid is supposed to interact with the two surfaces, the local dynamics changes with the distance z to each surface. We will treat the case of identical surfaces—more precisely identical surfaces and identical interaction layer-surface—separated by a viscous fluid. The extension to viscoelastic fluids is straightforward. Then we will propose an example of simplified gap composed of two homogeneous layers of brushes or irreversibly adsorbed chains (thickness e) separated from a liquid of free polymer chains by an interface of thickness ϵ. We will compare to a situation where the interfacial zones are replaced by two slipping planes. In Appendix B, we will consider how to generalize the analysis to asymmetric surfaces.

2.3.1. Expression of the Global Complex Modulus. Taking into account the variation of the viscosity with the distance z to the plane, the simplified motion equation is rewritten as

$$\frac{dP}{dr} = \frac{\partial}{\partial z}\left[\eta(z)\frac{\partial v_r}{\partial z}\right] \tag{11}$$

and the double integration gives rise to the expression of the total force on the plane (see Appendix A.II):

$$F(R, h_0, V) = 2\pi R^2 V \int_{h_0}^{\infty} dh \int_h^{\infty} \frac{dh}{\int_0^h dz \int_0^z \frac{h - 2z}{\eta(z)} dz} \tag{12}$$

By comparing it with eq 4, one deduces the experimental viscosity $\eta_{no}(h_0)$ of the gap for nonoverlapping layers. It is expressed as a function of the local viscosity $\eta(z)$ by

$$\eta_{no}(h_0) = \frac{h_0}{3} \int_{h_0}^{\infty} dh \int_h^{\infty} \frac{dh}{\int_0^h dz \int_0^z \frac{h - 2z}{\eta(z)} dz} \tag{13}$$

The extension to viscoelastic fluids submitted to small amplitude oscillations leads to

$$\eta_{no}^*(\omega, h_0) = \frac{h_0}{3} \int_{h_0}^{\infty} dh \int_h^{\infty} \frac{dh}{\int_0^h dz \int_0^z \frac{h - 2z}{\eta^*(\omega, z)} dz} \tag{14}$$

or, in terms of complex modulus

$$G^*_{no}(\omega, h_0) = \frac{h_0}{3}\int_{h_0}^{\infty} dh \int_h^{\infty} \frac{dh}{\int_0^h dz \int_0^z (h-2z)J^*(\omega, z)\, dz} \quad (15)$$

If we define an average complex compliance at distance r from the axis by

$$J^*(\omega, h) = \frac{6}{h^3}\int_0^h dz \int_0^z (h-2z)J^*(\omega, z)\, dz = \frac{1}{G^*(\omega, h)} \quad (16)$$

the global complex shear modulus can be expressed as a function of the semilocal one by

$$G^*_{no}(\omega, h_0) = 2h_0\int_{h_0}^{\infty} dh \int_h^{\infty} \frac{G^*(\omega, h)\, dh}{h^3} \quad (17)$$

Testing expression 15 supposes that one gives a physical meaning to the local variation of the viscoelastic behavior of the confined fluid. It is admitted that a brush behaves as an arm of star chain. The viscosity and the terminal relaxation time of entangled star polymers are much higher than those of linear chains of similar polymer with the same length.[20] Moreover, accurate velocimetry experiments[13] have proved that the interface between an entangled melt and a compatible brush exhibits a local friction which can be related to the modification of the local diffusion of the brush entangled with the melt. Therefore, we can model the gap by five symmetric layers: two brush layers, a central layer of free chains, and, inbetween that, two interfaces of thickness scaling as the interpenetration length.

2.3.2. A Five-Layer Picture. The layer parameters are as follows.

For the brushes: polymerization index N, thickness e, shear complex modulus $G^*_b(\omega)$ and compliance $J^*_b(\omega)$.

For the interfaces: thickness ϵ, shear complex modulus $G^*_{int}(\omega)$ and compliance $J^*_{int}(\omega)$.

For the free chains: polymerization index P, thickness $h - 2(e + \varepsilon)$, shear modulus $G^*_f(\omega)$, and compliance $J^*_f(\omega)$.

Due to the symmetry, the integration of eq 16 gives

$$J^*(\omega, h) = \frac{12}{h^3}\int_0^{h/2} dz \int_0^z (h-2z)J^*(\omega, z)\, dz = \frac{2}{h^3}\Big[(J^*_b - J^*_{int})(4e^2 - 6eh + 3h^2)e + (J^*_{int} - J^*_f)\{4(e+\varepsilon)^2 - 6h(e+\varepsilon) + 3h^2\}(e+\varepsilon) + \frac{1}{2}J^*_f h^3\Big] \quad (18)$$

and the global shear modulus is obtained by numerical integration of eq 17.

A lighting discussion of the above relation can be initiated by considering the case of large separations, i.e. e/h and $\varepsilon/h \ll 1$. The simplified expression of the semilocal shear modulus is

$$G^*(\omega, h) = \frac{1}{J^*(\omega, h)} \cong G^*_f(\omega)\left[1 - 6\left\{\left(\frac{G^*_f}{G^*_b} - 1\right)\frac{e}{h} + \left(\frac{G^*_f}{G^*_{int}} - 1\right)\frac{\varepsilon}{h}\right\}\right]$$

and the global shear modulus is (see relation 17):

$$G^*_{no}(\omega, h_0) = G^*_f(\omega)\left[1 - 4\left\{\left(\frac{G^*_f(\omega)}{G^*_b(\omega)} - 1\right)\frac{e}{h_0} + \left(\frac{G^*_f(\omega)}{G^*_{int}(\omega)} - 1\right)\frac{\varepsilon}{h_0}\right\}\right] \quad (19)$$

Therefore, the measured shear modulus can be different of that of free chains, even at large distances, if at least one of the two modulus ratios in the correcting factor is much higher than unity. For entangled chains, when $N \geq P > N_e$, G^*_f/G^*_b is much smaller than unity, and the leading term might be the last one

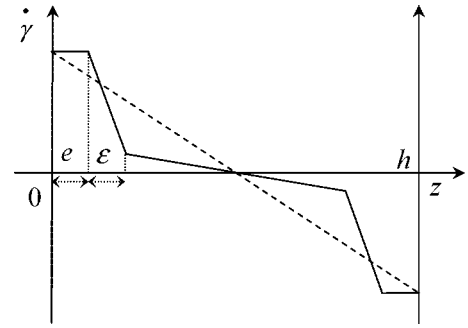

Figure 2. Shear rate profile for a gap of five homogeneous layers (solid line) compared to that of a homogeneous fluid (dotted line). In this example, the shear compliance of the interfaces is supposed to be higher than in free melt.

which accounts for the dynamics of the brush−melt interface. In other words, a sliding motion at the interface would lead to an underestimated shear modulus of free chains. It could be an explanation of shifts observed between bulk data and some measurements made at large separations with a dynamic surface force apparatus.[21] Before elaborating on the interpretation, we illustrate that situation by the radial velocity profile deduced from eqs A14 and A15 written as

$$v^*_r(\omega, r, z) = \frac{1}{2} rV^* \frac{\int_0^z (2z-h)J^*(\omega, z)\, dz}{\int_0^h dz \int_0^z (h-2z)J^*(\omega, z)\, dz} \quad (20)$$

from which we deduce the shear rate profile

$$\dot{\gamma}^*(z) = \frac{3rV^*}{h^3 J^*(h)}(2z-h)J^*(z) \quad (21)$$

and the five-layer description gives the following profile for the amplitude of the shear rate at a given frequency (Figure 2). The brushes almost do not participate in the shear flow, whereas the interfaces concentrate a large part of it.

2.3.3. Physical Interpretation. It is admitted that there is a great similarity between the dynamics of an end-grafted N chain (or a tail or loop of an irreversibly adsorbed chain) and of the arm of a star polymer. The tube model theory for star-shaped chains has been developed to a high degree of refinement.[22] It assumes that each arm renews its configuration by a retraction inside the tube via fluctuations until the end reaches the center of the star. That process leads to an exponential dependence of the relaxation time with N:

$$\lambda_{br} \propto \exp\left(\nu \frac{N}{N_e}\right)$$

The same dependence has been found for Langmuir monolayers of polyisoprene chains tethered by one end to the air−water interface.[23] The main result is an enhancement of both relaxation times and viscosity for about 2−3 orders of magnitude compared to bulk polyisoprene samples. The mass dependence is exponential as expected for branched chains. The authors conclude that arm retraction appears to be a relevant mechanism for their systems.

For a layer of grafted chains, the tube width is a function of the grafting density $\sigma = a^2/\Delta^2$. It varies like the distance Δ between grafting points. The brush length L depends also on the number P of monomers per free chain. Different regimes have been identified,[5] where the brush can be swollen by the melt and free chains are supposed to penetrate over the whole layer. At high density, one speaks of dry brush extended toward the melt and not interpenetrated by the P chains. Nevertheless, neutron reflexivity experiments[8] show a penetration of the P

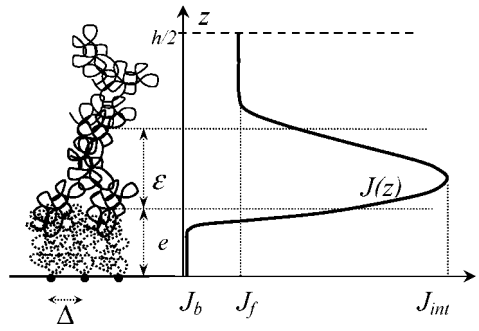

Figure 3. Shear compliance profile accounting for the interconnection between brushes and melt. Such overlapping modifies the local entanglement density within the interfaces. The shape of the curve accounts for a loss of entanglements of the free chains in contact with brushes. The subsequent faster tube renewal mechanism will spread over the gap at the scale of some free chains and defines an interface thickness ϵ.

chains over a distance l within the brush, due to the parabolic profile of the monomer concentration in the layer.[1] Then we can expect a brush−melt interface for almost all the combinations of parameters N, P, and σ.

Within the interface, the presence of P chains will affect the dynamics of each brush, therefore modifying the viscoelastic behavior of the first layer by a tube renewal process.[7] C. Gay[12] advocates that P chains spontaneously slide out from the N obstacles before they could be forced to do so by a shear flow, as supposed in the initial interfacial friction model.[24] Following the same lines, we postulate that as free P chains are diffusing not only by reptation but also by tube renewal, their diffusion will be affected by the interaction with brush ends.

Let us first remember the expressions of the main viscoelastic parameters of a melt of P entangled chains, given by the reptation models including tube renewal.[25−28]

Zero−shear viscosity:

$$\eta_0 \propto \frac{P^3}{N_e^{\,2}} \tag{22}$$

Steady−state compliance and rubbery plateau modulus:

$$J_0^e = \frac{1}{G_N^0} \propto N_e \tag{23}$$

Reptation time:

$$\lambda_{rep} \propto \frac{P^3}{N_e} \tag{24}$$

Tube renewal time:[27]

$$\lambda_{tube} \approx \frac{1}{28}\left(\frac{P}{N_e}\right)^2 \lambda_{rep} \tag{25}$$

Here N_e is the number of monomers between entanglements, and then P/N_e is the number of segments between entanglements.

If the total relaxation time is

$$\lambda^{-1} = \lambda_{rep}^{\ -1} + \lambda_{tube}^{\ -1} \tag{26}$$

then the faster mechanism will be dominant. From relation 25, the crossover occurs for $P \approx 5N_e$. Though there is a slight discrepancy between experimental data and the model,[29,30] the main conclusion holds: highly entangled chains mainly diffuse by reptation.

If we assume that the very mobile tail of each brush do not participate in the entanglement network, the tube of a P chain will be enlarged then N_e will be larger. The most favorable situation occurs when the penetration length l is equal to the tube diameter, i.e; $l_e^2 = N_e a^2$. For $l \gg l_e$, the brush participate in the entanglement network of the P chains and do not significantly modify the tube diameter. In the opposite situation, $l \ll l_e$, the P chains are mainly entangled with other P chains. For $l = l_e$, the entanglement density will be written as: $N_e' = N_e c^{-1}$where c is the fraction of P-monomers participating in the entanglement network. In a P melt, the number of monomers in a volume of R_g^3 is $P^{3/2}$. Within the same volume, the number of brushes is $R_g^2/\Delta^2 = P\sigma$, and then the number of N-monomers is $N_e P\sigma$.

Consequently, the fraction c is expressed by

$$c = 1 - \frac{\sigma N_e}{P^{1/2}} \tag{27}$$

The decrease of the entanglement density induces the following scaling laws for the above viscoelastic parameters:

$$\eta_0 \propto c^2\ ;\quad J_e^0 = G_N^{\ -1} \propto c^{-1}\ ;\quad \lambda_{rep} \propto c\ ;\quad \lambda_{tube} \propto c^3 \tag{28}$$

As generally $P < N_e^2$, the reduction of those parameters can be significant and justify that, even at large separations, the measured complex shear modulus can be shifted toward lower moduli and higher frequencies compared to the bulk modulus of P chains (eq 19).

Figure 3 summarizes the description of a symmetric gap. It gives a picture of the variation of the amplitude of the local complex compliance $J^*(\omega,z)$ at a given frequency. The brush layer exhibits high values of modulus (low value of compliance) and relaxation time like arms of star chains. P-chains are interconnected with the N-brushes, therefore decreasing the values (increasing J) until a distance corresponding to the mean position of the P-chains with a penetration length of l_e. The modification of the diffusion of P-chains continues as the faster motion of the P-chains in contact with the brush will have an effect on the other ones over a thickness ϵ. That description also holds for adsorbed layers for which the broad distribution of tails and loops will favor such an interfacial contribution.

2.3.4. Three Layers and Slipping Interface. An alternative vision of the friction between brush and melt has been proposed by Brochard and de Gennes.[24] It holds within a regime of shear velocity and tension where tethered chains are stretched. Therefore, at the interface, free P-chains exhibit a relative velocity or slipping velocity V_s compared to that of N-brushes. The initial forced sliding mechanism was demonstrated not adequate even at low velocities[12] and replaced by the concept of tube renewal. The tube of each grafted N-chain is progressively renewed as P-chains diffuse away and are replaced by other chains. Since the conformation of new chains is never identical to those of previous chains, the N-tube fluctuates. At low velocities, such fluctuations are equivalent to a friction force proportional to the sliding velocity V_s, and the extrapolation length b is constant.

In that regime, let us express the hydrodynamic force exerted on the plate for viscous and symmetric layers: viscosity η_b and thickness e for brushes and viscosity η_f for free chains. The extension to viscoelastic polymers will be straightforward.

From eqs A5 and A6 and incorporating the slipping velocity at the interface, the velocity profile is as follows.

For $0 < z < e$:

$$v_{r,b} = \frac{1}{2\eta_b}(z^2 - hz)\frac{dP}{dr} \tag{29}$$

For $e < z < h/2$:

$$v_{r,f} = \frac{1}{2\eta_f}\frac{dP}{dr}\left[z^2 - hz + \left(\frac{\eta_f}{\eta_b} - 1\right)(e^2 - he)\right] + V_s \tag{30}$$

The slipping velocity can be expressed as a function of the extrapolation length b by

$$V_s = b\left(\frac{\partial v_r}{\partial z}\right)_{z=e} = \frac{b}{2\eta_f}(2e-h)\frac{dP}{dr} \quad (31)$$

From eq A4, we deduce the pressure gradient

$$\frac{dP}{dr} = \frac{6\eta_f r V}{h^3 + 2\left(1-\frac{\eta_f}{\eta_b}\right)(4e^2-6eh+3h^2)e + 6b(h-2e)^2} \quad (32)$$

and finally, the hydrodynamic force:

$$F(R,h_0,V,b) = 12\pi R^2\eta_f V\int_{h_0}^{\infty} dh \times \int_h^{\infty} \frac{dh}{h^3 + 2\left(\frac{\eta_f}{\eta_b}-1\right)(4e^2-6eh+3h^2)e + 6b(h-2e)^2} \quad (33)$$

The generalization to viscoelastic gaps leads to

$$G^*(\omega,h_0,b) = 2h_0\int_{h_0}^{\infty} dh \times \int_h^{\infty} \frac{dh}{J_f^* h^3 + 2(J_b^*-J_f^*)(4e^2-6eh+3h^2)e + 6b(h-2e)^2} \quad (34)$$

That expression can be used for evaluating the extrapolation length and check its dependence on N, P, and σ. Moreover, it would be interesting to compare it to the predictions of the five-layer description (eqs 17 and 18) when the thickness ϵ of the interface tends to zero.

3. Overlapping Layers

When the separation h_0 between the two surfaces is lower than the thickness of the two layers, the tethered chains are compressed in the central zone ($h_0 < h(r) < h_1 = 2e$) and should behave as an elastic solid with a modulus E which varies with r. Oscillatory measurements conducted in that situation with adsorbed layers of polybutadiene[31] and with end-grafted polyacrylate brushes[21] exhibit a plateau modulus G_{pl} superimposed to the viscoelastic response observed for nonoverlapping layers (Figure 4).

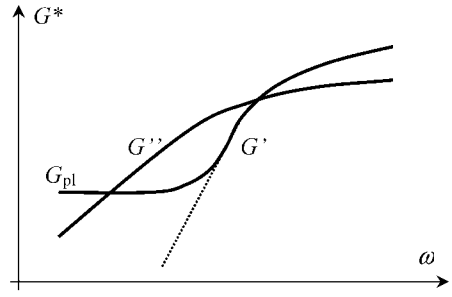

Figure 4. Sketch of experimental data of complex modulus for overlapping layers of adsorbed or grafted polymer chains. The plateau modulus G_{pl} accounts for the compression of the connected part of the layers.

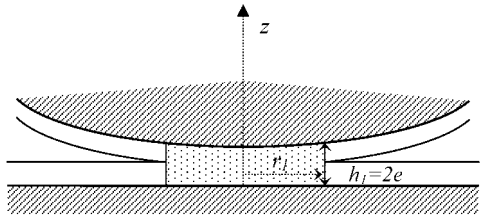

Figure 5. The overlapped layers occupy the central part of the gap until a distance r_l to the axis defined by a distance between the two surfaces of the order of twice the length of the tethered chains.

Such a plateau occurs in the terminal zone of the free chains; therefore, it is disconnected from the rubbery plateau generally observed with entangled polymers and attributed to the temporary entanglement network. We are going to establish a relation between the observed plateau G_{pl} and the local elastic modulus $E(r)$. Then, it will be integrated in the overall viscoelastic behavior of the gap sketched in Figure 5.>

3.1. Elastic Modulus. The force exerted on the plane by an axial motion U of the sphere is expressed by

$$F = \int_0^{r(h_1)} \tau_{zz}(z=0)\, 2\pi r\, dr = 2\pi R\int_{h_0}^{h_1} \tau_{zz}(z=0)\, dh \quad (35)$$

That component of the stress tensor obeys Hooke's law:

$$\tau_{zz} = (\lambda+2\mu)\,\varepsilon_{zz} + \lambda(\varepsilon_{rr}+\varepsilon_{\theta\theta})$$

λ and μ are Lame's coefficients.

For an axysymmetric geometry:

$$\tau_{zz} = \frac{E}{(1+\nu)(1-2\nu)}\left[(1-\nu)\,\partial_z u_z + \nu\,\frac{1}{r}\,\partial_r(ru_r)\right] \quad (36)$$

ν being Poisson's coefficient.

The strain $\mathbf{u} = [u_r(r,z), u_z(z)]$ obeys Navier's equations:

$$2(1-\nu)\,\partial_r\left[\frac{1}{r}\partial_r(ru_r)\right] + (1-2\nu)\,\partial_{zz}u_r + \partial_{rz}u_z = 0 \quad (37a)$$

$$\partial_z\left[\frac{1}{r}\partial_r(ru_r)\right] + (1-2\nu)\frac{1}{r}\partial_r(r\partial_r u_z) + 2(1-\nu)\partial_{zz}u_z = 0 \quad (37b)$$

The double integration of eq 37b with the condition of no slipping on the plane ($u_r(r,0) = 0$) and with $u_z(z)$ leads to

$$u_r(r,z) = -(1-\nu)r[\partial_z u_z - \partial_z u_z(z=0)] \quad (38)$$

The continuity for $r(h_1)$ imposes (see eq A8 for the radial velocity):

$$u_r = -\frac{3Ur}{h^3}z(h-z) \quad (39)$$

and, according to the boundary conditions: $u_z(0) = 0$ *et* $u_z(h) = U$, the axial deformation is

$$u_z = \frac{U}{2(1-\nu)}\left[(1-2\nu)\frac{z}{h} + 3\left(\frac{z}{h}\right)^2 - 2\left(\frac{z}{h}\right)^3\right] \quad (40)$$

which is compatible with expression A9 for the axial velocity of an incompressible system ($\nu = 1/2$).

Therefore, the normal stress to the plane is (eq 36):

$$\tau_{zz}(r,0) = \frac{E(r)}{2(1+\nu)}\frac{U}{h} = G(r)\frac{U}{h} \quad (41)$$

and, according to eq 35, the elastic force is:

$$F_{el}(R,h_0,U) = 2\pi RU\int_{h_0}^{2e}\frac{G(h)}{h}\,dh \quad (42a)$$

It is worth noting that the normal stress has the same expression as a shear stress with U/h being a tangential strain.

For small amplitude oscillations, the elastic force takes the same form as here above:

$$F_{el}^*(R,h_0,U^*) = 2\pi RU^*\int_{h_0}^{2e}\frac{G(h)}{h}\,dh \quad (42b)$$

This expression of the elastic force has to be compared with eq 10 which can be put in the following simplified form in the frequency range where the plateau modulus G_{pl} is detected:

$$F^*_{el}(R, h_0, U^*) = \frac{6\pi R^2 U^*}{h_0} G_{pl}(h_0) \quad (43)$$

Comparing eqs 42 and 43, we deduce that the local elastic modulus $E(h)$ due to the compression of the interpenetrated chains is directly connected to the measured plateau modulus G_{pl} by

$$E(h) = -6\,(1+\nu)R\left[\frac{\partial G_{pl}}{\partial h_0}\right]_{h_0=h} \quad (44)$$

As an example, let us report data from adsorbed layers of high polybutadiene[31] (weight-average molecular weight 330 000 g·mol^{-1}). Their thickness is about 25 nm and they are compressed until a separation of 39 nm. In that range of distances (39−50 nm), the average elastic modulus deduced from eq 44 is about 2×10^8 Pa, far beyond the rubbery plateau for free polybutadiene (around 10^6 Pa for the shear modulus).

Therefore, oscillatory experiments done with a surface force apparatus allow one to check the theories proposed in the literature for describing the change in chain conformation and the associated force profile when polymer layers are compressed. More often, this is done by means of the static force profile $F_{st}(h_0)$. As an example, in a recent paper,[32] Eiser et al. investigate the influence of free polymer chains on the equilibrium and dynamic properties of dense polymer brushes. They observe a strong influence of the free chains on the behavior of the brushes when high shear rates are applied, even when the brushes are well away from contact, indicating a clear coupling between the brushes and the free polymer.

We have proved[31] that the relation between the static force and the dynamic one is simply

$$F_{el} = -U\frac{\partial F_{st}}{\partial h_0} \quad (45)$$

but the oscillatory force produced by a small perturbation around equilibrium not only provides an elastic force but also provides a hydrodynamic one, accounting for the shear solicitation of the gap.

3.2. Overall Behavior. The elastic force exerted by the central zone of the gap is added to the viscoelastic force due to the shear of the surrounding fluid made of noninterconnected layers and of free chains. In other words, the low frequency plateau modulus is superimposed to the relaxation spectrum of tethered and free chains. Indeed, the central part is submitted to a shear field and will contribute to the viscoelastic part of the force. Its contribution is a complex viscosity or modulus controlled by the degree of overlapping, i. e. $\eta^*_{ov}(h)$. At the boundary $h_1 = 2e$, the layers are just in contact, and then $\eta^*_{no}(2e) = \eta^*_{ov}(2e) = \eta^*(2e)$.

The corresponding force $F_c^*(R, h_0, \omega)$ is derived from eq A7

$$\frac{dP^*}{dr} = \frac{6\eta^*_{ov}(\omega, h)\dot{U}}{h^3} r$$

integrated until $h = 2e$, where

$$P^*(2e) = \frac{3R\eta^*(\omega, 2e)\dot{U}}{4e^2}$$

Then, the resulting hydrodynamic force in the central zone will be

$$F^*_{ov}(R, h_0, \omega) = 12\pi R^2 \dot{U}\int_{h_0}^{2e} dh \int_h^{2e} \frac{\eta^*_{ov}(\omega, h)}{h^3}\, dh + \frac{3\pi R^2 \dot{U}\eta^*(\omega, 2e)}{2e^2}(2e - h_0) \quad (46)$$

which represents the complex shear modulus of the overlapped layers:

$$G^*_{ov}(R, h_0, \omega) = 2h_0\int_{h_0}^{2e} dh \int_h^{2e} \frac{G^*_{ov}(\omega, h)}{h^3}\, dh + \frac{G^*(\omega, 2e)}{4e^2}(2e - h_0)h_0 \quad (47)$$

The overall complex force throughout the gap is obtained by summing the three contributions: the viscoelastic force of the inner part (eq 46), the viscoelastic force of the outer part (eq 12 put in a complex form and limited to the range $h > 2e$) and the elastic force (eq 42b), i.e.

$$F^*(R, h_0, \omega) = 12\pi R^2 \dot{U}^* \int_{h_0}^{2e} dh \int_h^{2e} \frac{\eta^*_{ov}(\omega, h)}{h^3}\, dh + \frac{3\pi R^2 \dot{U}^* \eta^*(\omega, 2e)}{2e^2}(2e - h_0) + 2\pi R^2 \dot{U}^* \int_{2e}^{\infty} dh \int_h^{\infty} \times \frac{dh}{\int_0^h dz \int_0^z \frac{h - 2z}{\eta^*_{no}(\omega, z)}\, dz} + 2\pi R U^* \int_{h_0}^{2e} \frac{G(h)}{h}\, dh \quad (48)$$

which expresses the measured complex modulus for $h_0 < 2e$:

$$G^*(R, h_0, \omega) = 2h_0\int_{h_0}^{2e} dh \int_h^{2e} \frac{G^*_{ov}(\omega, h)}{h^3}\, dh + \frac{G^*(\omega, 2e)}{4e^2}(2e - h_0)h_0 + \frac{h_0}{3}\int_{2e}^{\infty} dh \int_h^{\infty} \frac{dh}{\int_0^h dz \int_0^z (h - 2z) J^*_{no}(\omega, z)\, dz} + \frac{h_0}{3R}\int_{h_0}^{2e} \frac{G(h)}{h}\, dh \quad (49)$$

The last term is purely elastic; it accounts for the low frequency plateau modulus G_{pl}. Its profile provides information about the elastic modulus $E(h)$ due to the compression of the layers (eq 44). The contribution of the second and third terms can be deduced from measurements at large surface separation ($h_0 \geq 2e$). They describe the viscoelastic behavior of layers separated by free chains. By subtracting those three terms from the experimental data, one isolates the shear contribution $G^*_{ov}(\omega, h_0)$ of the inner part. Then, the variation of the local shear modulus can be expressed by

$$G^*_{ov}(\omega, h) = h^3\left[\frac{\partial^2}{\partial h_0}\left(\frac{G^*_{ov}(\omega, h_0)}{2h_0}\right)\right]_{h_0=h} \quad (50)$$

As a summary, the harmonic force measured when exploring the sphere−plane gap around equilibrium provides the most complete information about the dynamics of polymer chains confined the gap. From the variations of the measured parameters—elastic modulus, viscosity, and shear modulus—with separation h_0 we have an access to the corresponding local quantities.

The local elastic modulus is given in eq 44.

The semilocal complex shear modulus of nonoverlapped layers and free chains can be expressed from eq 17 by

$$G^*_{no}(\omega, h) = h^3\left[\frac{\partial^2}{\partial h_0}\left(\frac{G^*_{no}(\omega, h_0)}{2h_0}\right)\right]_{h_0=h} \quad (51)$$

The local complex shear modulus of overlapped layers is given by eq 50.

It is also possible to go back to the local behavior of nonoverlapped layers via eq 16 which can be written as:

$$J^*_{no}(\omega, z) = -\frac{1}{z}\left[\frac{\partial^2}{\partial h^2}\left(\frac{h^3}{6G^*_{no}(\omega, h)}\right)\right]_{h=z} \quad (52)$$

4. Conclusion

We have demonstrated that dynamic surface force apparatuses are tools appropriate for investigating the details of the rheology

of polymer systems confined between a plane and a sphere. In the framework of Derjaguin's approximation, the shear stress field within the gap has been established by considering a variation of the local properties with the distance to the substrates. Such approximation imposes that the radius of the sphere is much larger than the surface separation. As atomic force microscopes are also used for investigating confined fluids, it is worth knowing that such technique does not comply with Derjaguin's approximation unless a large enough sphere is fixed to the tip. Harmonic axial motions of very small amplitude act as a probe of the equilibrium properties of the fluid. Consequently, we are dealing with linear viscoelasticity which implies that the viscoelastic parameters are not stress-dependent. Moreover, the mechanical response of the equipment has to be well separated from that of the sample. That condition is usually fulfilled by indentation technology which exhibits a high level of rigidity and a resonance frequency out of the range of the characteristic times of polymer melts. Obviously, the raw data have to be corrected by the device response.

We have focused this paper on polymer melts or concentrated solutions interacting with adsorbed or grafted polymer chains. We have proposed a method of data analysis which discriminates the distinct contributions coming from the free and the tethered chains. For doing so, a sufficient number of experiments have to be conducted in the widest range of surface separation from infinity to near contact, those notions being dictated by molecular size. From that distance scan, it is possible to deduce the local viscoelastic parameters with a good accuracy (eqs 44, 50, 51, and 52). A loss of precision can originate in the surface roughness. Mica sheets or silicon wafers are molecularly smooth but other types of substrate can induce a notable perturbation of the film thickness. That would mainly affect the contribution of the free chains, at least at large separation.

We have deeply analyzed the interaction between similar surfaces, nevertheless the description of non identical surfaces (see Appendix B) should be useful for investigating, for example, the bridging of chains between a covered surface and a bare one. It is worth noting that one has to choose a large frequency sweep for describing not only the terminal zone of chain relaxation, either free or tethered, but also the segmental motions of the chains.

That would be of great help for exploring the overlapping zone between free and trapped chains. Such experiments should bring an interesting material for testing molecular models of interfacial friction. The good control of living radical polymerization techniques provides well-defined layers of end-grafted chains, in terms of chain length, narrow length distribution, and grafting density. Therefore, experimentalists can play around, matching the characteristics of brushes with those of free polymer chains: molecular weight, linear or branched architectures, compatibility, and solvent concentration. The continuous refinements of reptation models provide analytical expressions of shear modulus for various architectures. They can be used for interpretation of the dynamics of entangled chains.

Out of interest, all the results presented in this paper are transposable to sphere−sphere interactions by multiplying by a factor of 2. The link is obvious with applications dealing with concentrated suspensions of spheres for which the radius is much higher than the distance between them. Surface treatments by means of macromolecules compatible or not with the surrounding fluid are of paramount importance for the mechanical properties of the material.

Appendix A

I. Lubrication Force for Homogeneous and Newtonian Fluids The basic equations are as follows.

The constitutive equation:

$$\tau_{rz} = \eta \frac{\partial v_r}{\partial z} \tag{A1}$$

The motion equation:

$$\frac{dP}{dr} = \eta \frac{\partial^2 v_r}{\partial z^2} \tag{A2}$$

The continuity equation:

$$\frac{1}{r}\frac{\partial}{\partial r}(r v_r) + \frac{\partial v_z}{\partial z} = 0 \tag{A3}$$

The integration of eq A3 leads to

$$\int_0^r \frac{\partial}{\partial r}(r v_r)\, dr = -\int_0^r r \frac{dv_r}{dz}\, dr$$

that is

$$v_r = -\frac{1}{2} r \frac{dv_z}{dz}$$

and a second integration gives

$$\int_0^h v_r\, dz = -\frac{1}{2} r \int_0^h \frac{dv_z}{dz}\, dz = -\frac{1}{2} rV(t) \tag{A4}$$

From the integration of eq A2

$$\eta \frac{\partial v_r}{\partial z} = z\frac{dP}{dr} + a(r) \tag{A5}$$

The symmetry between the two surfaces gives $(\partial v_r/\partial z)_{z=h/2} = 0$ which leads to $a(r) = -(h/2)(dP/dr)$. And assuming no slippage at the surfaces, the radial velocity profile is

$$v_r = \frac{1}{2\eta}(z^2 - hz)\frac{dP}{dr} \tag{A6}$$

Coupling it with eq A4

$$\frac{dP}{dr} = \frac{6\eta r V}{h^3} \tag{A7}$$

from which we can express the velocity field

$$v_r = 3V\frac{r(z^2 - hz)}{h^3} \tag{A8}$$

$$v_z = -\frac{V}{h^3}(2z^3 - 3hz^2) \tag{A9}$$

and the total force acting on the plane

$$P(r) - P(\infty) = 6\eta V \int_\infty^r \frac{r}{h^3}\, dr = 6\eta R V \int_\infty^h \frac{1}{h^3}\, dh = -\frac{3\eta R V}{h^2} \tag{A10}$$

$$F(R, h_0, V) = 2\pi \int_0^\infty [\tau_{zz} - P(r) + P(\infty)]_{z=0}\, r\, dr = \frac{6\pi R^2 \eta V}{h_0} \tag{A11}$$

II. Lubrication Force for Heterogeneous and Newtonian Fluid. Assuming that the viscosity varies with z, the motion equation is modified in that way:

$$\frac{dP}{dr} = \frac{\partial \tau_{rz}}{\partial z} = \frac{\partial}{\partial z}\left[\eta(z)\frac{\partial v_r}{\partial z}\right] \tag{A12}$$

By integration

$$\eta(z)\frac{\partial v_r}{\partial z} = z\frac{dP}{dr} + a(r) \tag{A13}$$

and the symmetry still imposes

$$a(r) = -\frac{h}{2}\frac{\mathrm{d}P}{\mathrm{d}r}$$

from which we deduce

$$v_r(r,z) = \frac{\mathrm{d}P}{\mathrm{d}r}\int_0^z \frac{2z-h}{2\eta(z)}\,\mathrm{d}z \tag{A14}$$

As the continuity equation eq A3 is not affected by the viscosity variations, the coupling of eqs A4 and A14 gives the pressure gradient:

$$\frac{\mathrm{d}P}{\mathrm{d}r} = \frac{Vr}{\int_0^h \mathrm{d}z \int_0^z \frac{h-2z}{\eta(z)}\,\mathrm{d}z} \tag{A15}$$

The lubrication force is obtained by a double integration and is expressed by

$$F(R,h_0,V) = 2\pi R^2 V \int_{h_0}^{\infty}\mathrm{d}h \int_h^{\infty} \frac{\mathrm{d}h}{\int_0^h \mathrm{d}z \int_0^z \frac{h-2z}{\eta(z)}\,\mathrm{d}z} \tag{A16}$$

Appendix B: Asymmetric Surfaces

The modifications arising from the asymmetry of the gap appear in eq A13:

$$\eta(z)\frac{\partial v_r}{\partial z} = z\frac{\mathrm{d}P}{\mathrm{d}r} + a(r)$$

The factor $a(r)$ is obtained by integration over the gap, without slippage at the surfaces

$$\int_0^h \frac{\partial v_r}{\partial z}\,\mathrm{d}z = 0 = \frac{\mathrm{d}P}{\mathrm{d}r}\int_0^h \frac{z}{\eta(z)}\,\mathrm{d}z + a(r)\int_0^h \frac{1}{\eta(z)}\,\mathrm{d}z$$

then

$$a(r) = -\frac{\mathrm{d}P}{\mathrm{d}r}\frac{\int_0^h \frac{z}{\eta(z)}\,\mathrm{d}z}{\int_0^h \frac{1}{\eta(z)}\,\mathrm{d}z}$$

which defines a distance $h_{\eta^{-1}}$weighted by the reciprocal of the viscosity:

$$h_{\eta^{-1}} = \frac{\int_0^h \frac{2z}{\eta(z)}\,\mathrm{d}z}{\int_0^h \frac{1}{\eta(z)}\,\mathrm{d}z} \tag{B1}$$

It follows that, for a viscous heterogeneous fluid, all the subsequent expressions are identical as for symmetric surfaces, changing the real distance h by the modified one $h_{\eta^{-1}}$.

The generalization to a viscoelastic heterogeneous fluid is straightforward:

$$h_J^* = \frac{\int_0^h 2zJ^*(\omega,z)\,\mathrm{d}z}{\int_0^h J^*(\omega,z)\,\mathrm{d}z} \tag{B2}$$

and that expression must replace h in eqs 14 and 15.

Moreover, the radial velocity will be expressed by

$$v_r^*(r,z) = -\frac{1}{2}V^* r\frac{\int_0^z (h_J^*-2z)J^*(\omega,z)dz}{\int_0^h dz\int_0^z (h_J^*-2z)J^*(\omega,z)dz} \tag{B3}$$

At low separations, when two different layers are overlapped or when a unique layer is bridging the two surfaces, the solution is the same for the shear complex modulus as for large separations. The elastic modulus is supposed to depend on both variables, $E(r,z)$, at least for weakly connected layers. Assuming that the axial displacement is mainly a function of z, i.e., $u_z(z)$, the solution of eq 37b is identical (eq 38) with u_r expressed by

$$u_r^*(r,z) = -\frac{1}{2}U^* r\frac{\int_0^z (h_J^*-2z)J^*(\omega,z)\,\mathrm{d}z}{\int_0^h \mathrm{d}z\int_0^z (h_J^*-2z)J^*(\omega,z)\,\mathrm{d}z} \tag{B4}$$

Equation 38 can be integrated over z

$$(1-\nu)[u_z^* - z[\partial_z u_z^*]_{z=0}] = \frac{1}{2}U^*\frac{\int_0^z \mathrm{d}z\int_0^z (h_J^*-2z)J^*(\omega,z)\,\mathrm{d}z}{\int_0^h \mathrm{d}z\int_0^z (h_J^*-2z)J^*(\omega,z)\,\mathrm{d}z}$$

and the boundary condition $u_z(h) = U$ gives directly

$$(1-\nu)[\partial_z u_z^*]_{z=0} = \frac{1-2\nu}{2}\frac{U^*}{h}$$

Then, from eq 36, the compression stress on the plane is

$$\tau_{zz}^* = \frac{E(r,0)}{2(1+\nu)}\frac{U^*}{h} \tag{B5}$$

and the elastic force has the same expression as for symmetric gaps (eq 41). The only difference is that the value of the elastic modulus close to the plane depends on the chain conformation. The problem is simpler for strongly overlapped layers for which one can assume a constant modulus.

Acknowledgment. We thank Christophe Derail for bringing to us interesting light on some unexpected features of experimental data. We are grateful to Cyprien Gay for stimulating discussions about chain dynamics at the interface.

Note Added After ASAP Publication. This article was published ASAP on May 17, 2008. The name of the author in ref 21 was spelled incorrectly. The correct version was published on June 6, 2008.

References and Notes

(1) Milner, S. T.; Witten, T. A.; Cates, M. E. *Macromolecules* **1988**, *21*, 2610–2619.
(2) de Gennes, P. G. *Macromolecules* **1981**, *14*, 1637–1644.
(3) Guiselin, O. *Europhys. Lett.* **1992**, *17*, 225–230.
(4) de Gennes, P. G. *Macromolecules* **1980**, *13*, 1069–1075.
(5) Aubouy, M.; Fredrickson, G. H.; Pincus, P. A.; Raphael, E. *Macromolecules* **1995**, *28*, 2979–2981.
(6) Leibler, L.; Adjari, A.; Mourran, A.; Coulon, G.; Chatenay D. *In the Proceedings of the International Conference on Ordering in Macromolecular Systems*; Springer Verlag: Berlin, 1994.
(7) Gay, C. *Macromolecules* **1997**, *30*, 5939–5943.
(8) Marzolin, C.; Auroy, P.; Deruelle, M.; Faulkers, J. P.; Léger, L.; Menelle, A. *Macromolecules* **2001**, *34*, 8694–8700.
(9) Hoy, R. S.; Grest, G. S. *Macromolecules* **2007**, *40*, 8389–8395.
(10) Fredrickson, G. H.; Pincus, P. A. *Langmuir* **1991**, *7*, 786–795.
(11) Sens, P.; Marques, C. M.; Joanny, J. F. *Macromolecules* **1994**, *27*, 3812–3820.
(12) Gay, C. *Eur. Phys. J.* **1999**, *B 7*, 251–262.
(13) Durliat, E.; Hervet, H.; Léger, L. *Europhys. Lett.* **1997**, *38*, 383–388.
(14) Luckmam, P. F.; Manimaaran, S *Adv. Colloid Interface Sci.* **1997**, *73*, 1–46.
(15) Tonck, A., *Ph.D. Thesis Ecole Centrale de Lyon*, 1989.
(16) Hu, H. W.; Granick, S. *Science* **1992**, *258*, 1339–1342.

(17) Chan, D. Y. C.; Horn, R. G. *J. Chem. Phys.* **1985**, *83*, 5311–5324.
(18) Vinogradova, O. I. *Colloid J.* **1996**, *5*, 557–560.
(19) Montfort, J. P.; Hadziioannou, G. J. *J. Chem. Phys.* **1988**, *88*, 7187–7196.
(20) Roovers, J. *Macromolecules* **1991**, *24*, 5895–5896.
(21) Guatarbes B. Ph.D. Thesis, Université de Pau et des Pays de l'Adour, 2006.
(22) Milner, S. T.; McLeish, T. C. B. *Macromolecules* **1997**, *30*, 2159–2166.
(23) Luap, C.; Goedel, W. A. *Macromolecules* **2001**, *34*, 1343–1351.
(24) Brochard-Wyart, F.; de Gennes, P. G. *Langmuir* **1992**, *8*, 3033–3037.
(25) Doï, M.; Edwards, S. F. *J. Chem. Soc.* **1978**, *74*, 1789–1833. Doï, M.; Edwards, S. F. *J. Chem. Soc.* **1979**, *75*, 38–55.
(26) Klein, J. *Macromolecules* **1978**, *11*, 852–858.
(27) Daoud, M.; de Gennes, P. G. *J. Polym. Sci., Phys. Ed.* **1979**, *17*, 19711981.
(28) Graessley, W. W. *Adv. Polym. Sci.* **1982**, *47*, 67–117.
(29) Montfort, J. P.; Marin, G.; Monge, P. *Macromolecules* **1984**, *17*, 1551–1560.
(30) Roovers, J. *Macromolecules* **1987**, *20*, 148–152.
(31) Pelletier, E.; Montfort, J. P.; Loubet, J. L.; Tonck, A.; Georges, J. M. *Macromolecules* **1995**, *28*, 1990–1995.
(32) Eiser, E.; Klein, J. *Macromolecules* **2007**, *40*, 8455–8463.

MA7028488